

Flexible fabrication of microlens array surface on mold steel by magnetic field-assisted self-assembly electrode

K.S. Li^{1,2}, C.J. Wang^{1,#}, C.F. Cheung¹, F. Gong²

¹ State Key Laboratory of Ultra-precision Machining Technology, Department of Industrial and Systems Engineering The Hongkong Polytechnic University, Hong Kong, China

² Shenzhen Key Laboratory of High Performance Nontraditional Manufacturing, College of Mechatronics and Control Engineering Shenzhen University Shenzhen, Guangdong, China

[#] Corresponding Author / Email: chunjin.wang@polyu.edu.hk, TEL: +81-222-33-4444, FAX: +1-222-33-4444

KEYWORDS: Mold steel; microlens array surface; electrical discharge machining; self-assembly electrode

Mold steel, like H13 and M2, are widely used in critical industrial applications due to their excellent wear resistance and thermal hardness. Electrical discharge machining (EDM) is an effective method for fabricating structured surfaces on conductive materials. However, significant electrode wear and a complex replacement process result in high fabrication costs and low production efficiency. Therefore, EDM with a magnetic field-assisted self-assembly electrode (MASAE) was proposed for creating microlens array surfaces on H13. However, significant electrode wear and a complex replacement process result in high fabrication costs and low production efficiency. Therefore, EDM with a self-assembly electrode was proposed for creating microlens array surfaces on H3 mold steel. The MASAE consists of an array of ferromagnetic metallic balls held together by a magnetic field from a permanent magnet. By adjusting the position, number, and size of the metallic balls, various MASAEs can be created. After the EDM process, various microlens arrays on H13 can be fabricated. The shape evolution and surface roughness of the microlens array were investigated by ContourGT-X 3D optical profile and scanning electron microscope (SEM). The results indicate that self-assembling ball electrodes offer significant advantages in machining microlens array structure.

1. Introduction

Mold steel is a high-quality carbon and alloy steel specifically designed for manufacturing tools, and molds used in various industrial processes. With its high hardness, wear resistance, and ability to maintain a sharp cutting edge at elevated temperatures, mold steel is crucial for precision machining and shaping applications. Electrical discharge machining (EDM), a non-conventional process, is an effective method for machining conductive materials, unaffected by the material's composition, hardness, strength, or ductility [1-3]. In the EDM process, the design and preparation of electrodes are crucial for machining efficiency, cost, and the final shape of the workpiece. In recent years, researchers have developed various novel electrodes, such as rotary dentate disk foil electrodes [4], long-laminated electrodes [5], wheel-shaped rotary cupronickel electrodes [6], and self-assembly sheet electrodes [7]. By designing and optimizing electrodes during the EDM process, functional structured array surfaces can be fabricated with high efficiency and low worn.

Che et al. [8] used ultrasonic vibration-assisted EDM for the 45# steel. The results showed that the surface roughness of the workpiece was improved from 2.543 μm to 2.050 μm with the assistance of

ultrasonic vibration and the material removal rate increased nearly three times compared with traditional EDM. Gu et al. [9] presented a bundled die-sinking electrode designed to achieve high-performance and cost-efficient EDM of Ti6Al4V alloys. Song et al. [10] proposed using strip electrodes to create a square structure array on 304 stainless steels. The continuous rolling of strip electrodes reduces wear and enhances machining accuracy. For the fabrication of microlens arrays mold, Takino et al. [11] proposed a ball-type electrode that secured by a mechanical structure and spring. However, the ball-type electrode has disadvantages in clamping and replacement. Therefore, optimizing the electrode design is crucial for the EDM process [12-14].

In this paper, a novel MASAE is proposed for manufacturing of microlens array surface on H13 mold steel. The MASAE method involves using a magnet to adsorb discrete balls. By adjusting the sizes of the magnet and balls, electrodes of various scales can be fabricated. The surface roughness of the lens array surface was analyzed by measuring the arithmetic average height (S_a) and maximum peak height (S_p). The shape evolution and microstructures of the EDMed workpiece was observed by a white light profilometer and SEM. Finally, the discharge characteristic of MASAE was revealed.

2. Methods

2.1 Design and manufacture of MASAE

Fig. 1(a) shows the schematic of the mold geometry. The D and H is the diameter and height of single lens, respectively. I is the spacing between array. Fig. 1(b) shows the schematic of a self-assembly ball electrode. A self-assembled ball electrode is composed of magnet spheres utilizing the magnetic force of a permanent magnet. By adjusting the arrangement and size of the spheres, various self-assembled electrodes can be created.

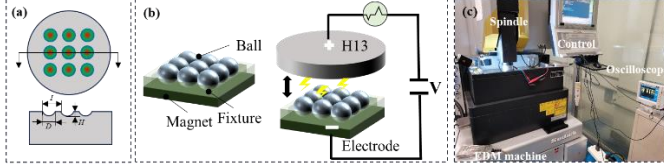


Fig. 1 (a) The schematic of the mold geometry, (b) The schematic of EDM with MASAE, (c) Experimental setup.

2.2 Experimental section

The experiments were performed using a three-axis Sodick electrical discharge machine (model APIL), as shown in Fig. 1(c). H13 mold steel (4Cr5MoSiV1) was selected as the workpiece materials. Pulse discharge energy was applied between the electrodes and the workpiece, transferring the surface structures of the self-assembled electrodes onto the machined workpiece. The EDM conditions and electrode properties are summarized in Table 1.

Table 1 EDM conditions

Conditions		Value
Processing parameters	Input current (A)	0.5
	Pulse width (μs)	1/5/10
	Pulse interval (μs)	5
	Open voltage (V)	105
	Dielectric fluid	Discharge oil
Tool electrodes	Tool diameter (mm)	1/3/5
	Resistivity ($\Omega\cdot\text{m}$)	2×10^{-7}
	Magnet (T)	1.1

2.3 Characterization

The surface roughness and shape evolution of the structured surface were assessed using a ContourGT-X 3D optical profiler (Bruker, Germany). The microstructure and subsurface damage of the EDMed workpiece were observed using (SEM, FEI, QUANTA FEG 450). The composition changes of the EDMed surface were analyzed using energy dispersive X-ray spectroscopy (EDS, FEI, QUANTA FEG 450).

3. Results and discussion

Fig. 2 shows the surface quality analysis of the EDMed H13 mold steel. By adjusting the MASAE and discharge parameters, array structure on H13 mold steel is fabricated, as shown in Fig. 2(a). Fig. 2(b) shows the SEM image of the EDMed surface. During the discharge process, a plasma channel forms at the interface between the workpiece and the electrode, generating an ultra-high instantaneous

temperature that causes the workpiece to melt and vaporize. After EDM, the surface will have small pits caused by discharge sparks, leading to increased surface roughness, as shown in Figs.2 (b) and (c). At the conditions of 0.5A/5 μs /10 μs , the S_a is about 0.65 μm . Fig.2 (d) shows the S_a of the EDMed surface at different conditions. Surface roughness depends on machining parameters like discharge energy and pulse duration. Rougher surfaces are common in roughing operations, while smoother surfaces can be achieved in finishing operations. As the pulse width reduces, smaller micro-craters develop on the fabricated surfaces, leading to lower surface roughness. When the pulse width, interval, and current are 1 μs , 5 μs , and 0.5 A respectively, the S_a value of the EDMed WC surface approximates to 0.23 μm .

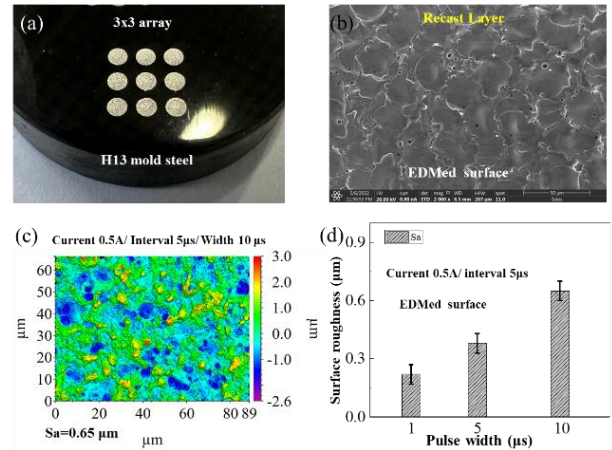


Fig. 2 The surface quality of the EDMed workpiece, (a) The image of H13 3 \times 3 array mold, (b) The SEM image of the EDMed surface, (c) The surface morphology of the EDMed surface, (d) The surfaces roughness of the EDMed surface at different pulse width.

Fig. 3(a) shows the surface morphology of 3 \times 3 lens array made by MASAE. The diameter (D) and depth (H) of the H13 mold after EDM are about 1.25 mm and 230 μm , respectively. Fig. 3(b) shows the material removal rate (MRR), and tool wear ratio (TWR) during the EDM process. When pulse widths are 1, 5, and 10 μs , the MRR are about 0.082 mm³/min, 0.13 mm³/min, and 0.21 mm³/min under a constant pulse current of 0.5 A and pulse interval of 10 μs . In certain cases, the MRR and TWR increase as the pulse width increases.

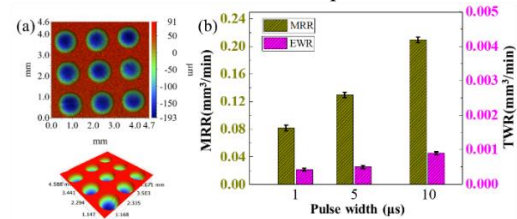


Fig. 3 (a) The morphology of 3 \times 3 lens array structures, (b) The MRR and TWR during EDM process.

Fig.4 shows the SEM image of the EDMed interface. Some surface cracks and holes can be observed from the high-resolution SEM image. The high temperatures during EDM can cause localized melting and rapid solidification of the material, leading to the formation of microcracks on the surface. EDM frequently generates a thin recast layer on the surface, commonly referred to as the “white layer.” This layer forms when the material melts during machining and then

resolidifies on the surface. The white layer is usually harder than the base material but also more brittle, increasing the likelihood of microcrack formation. Besides, surface cracks may extend into the subsurface, and pores can also form beneath the recast layer.

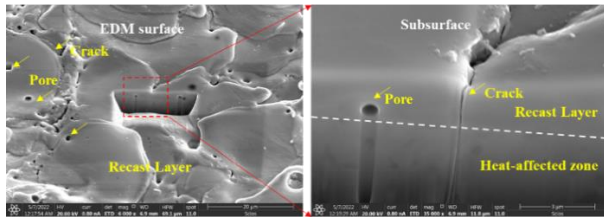


Fig. 4 The subsurface characteristic of the EDMed H13 mold

Fig. 5 shows EDS of the H13 mold steel before and after EDM. During EDM, the carbon content at the surface of H13 tool steel may fluctuate due to the high-temperature sparks. The high temperatures and rapid cooling in EDM can cause alloying elements (like Cr and Mo) to migrate and diffuse within the surface layer, leading to a composition gradient between the surface and the bulk material. EDM significantly alters the composition and microstructure of H13 tool steel, particularly at the surface. These changes, including variations in carbon content, elemental migration, and the formation of a recast layer, can affect the material's performance in critical applications.

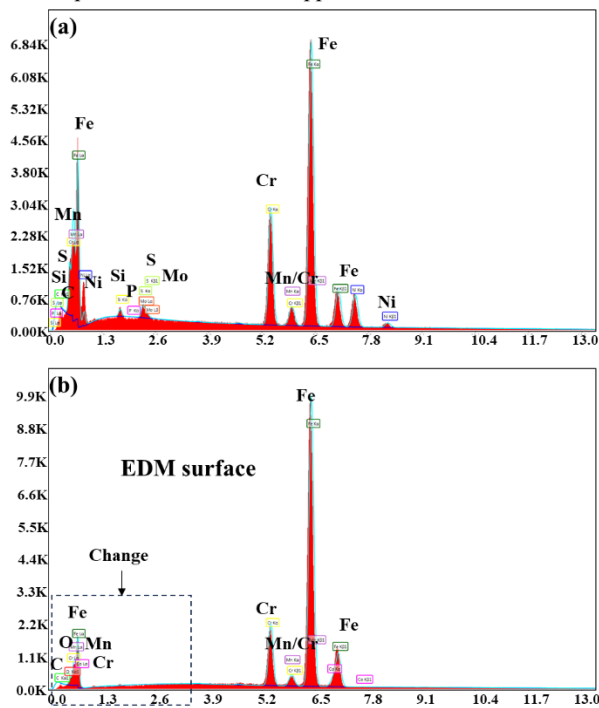


Fig. 5 The composition changes of the EDMed H13 surface, (a) Before EDM, (b) After EDM.

4. Conclusions

In this paper, a novel MASAE for EDM of the structured array on H13 mold steel is presented. MASAEs offer significant advantages over traditional integral electrodes made by milling or turning, particularly in fabricating structured array surfaces on conductive substrates. Higher pulse energy can enhance machining efficiency and MRR during EDM, but it also causes larger craters, increasing surface

roughness. After EDM, surface composition and microstructure of the H13 mold steel have significant changes due to the high-energy discharges and thermal effects. The work provides an effective method for manufacturing of the surface structure array on the WC.

ACKNOWLEDGEMENT

The work described in this paper was mainly supported by a Shenzhen-Hong Kong-Macau Technology Research Programme from Shenzhen Science and Technology Innovation Committee (Project No: SGD20220530110804030), the Research and Innovation Office of The Hong Kong Polytechnic University (Project code: BBR8 and BBX5), and Postdoctoral Matching Fund Scheme (1-W340). In addition, the authors would like to express their sincere thanks to the funding support from the Innovation and Technology Commission (ITC) of the Government of the Hong Kong Special Administrative Region (HKSAR), China (Project code: GHP/142/19SZ).

REFERENCES

- Li, K., Wang, C., Gong, F., Cheung, C. Facile and flexible fabrication of structured array surfaces on binderless tungsten carbide by using electrical discharge machining with a novel self-assembly ball electrode. *J. Am. Ceram. Soc.* Vol. 106, pp. 7386-99, 2023.
- Jithin, S., Joshi, S. Surface topography generation and simulation in electrical discharge texturing: A review. *J Mater. Process. Tech.*, Vol. 298, pp. 117297, 2021.
- Ming, W., Xie, Z., Du J., Zhang, G., Cao, C., Zhang, Y. Critical review on sustainable techniques in electrical discharge machining, *J Manu. Process.*, Vol. 72, pp. 375-99, 2021.
- Wu, W., Wu, X., Lei, J., Xu, B., Jiang, K., Wu, Z. Fabrication of deep-narrow microgrooves by micro-EDM using rotary dentate disc foil electrodes in emulsion. *J. Micromech. Microeng.* Vol. 29, pp. 035014, 2019.
- Lei, J., Wu, X., Zhou, Z., Xu, B., Tang, Y. Sustainable mass production of blind multi-microgrooves by EDM with a long-laminated electrode. *J. Clean. Prod.* Vol. 279, pp. 123492, 2020.
- Yan, J., Watanabe, K., Aoyama, T. Micro-electrical discharge machining of polycrystalline diamond using rotary cupronickel electrode. *CIRP Annals – Manuf. Tech.* Vol. 63, No. 1, pp.209-212, 2014.
- Li, K., Wang, C., Gong, F., Cheung, C., Chen, Z., Wang, Z. Coating-Free Superhydrophobic Hard Surfaces by Electric Discharge Machining with a Magnetic-Assisted Self-Assembly Sheet Electrode. *ACS Appl. Mater. Interfaces* Vol. 16, No. 12, pp. 15548–15557, 2024.
- Che, J., Zhou, T., Zhu, X., Kong, W., Wang, Z., Xie, X. Experimental study on horizontal ultrasonic electrical discharge machining. *J. Mater. Process. Tech.* Vol. 231, pp. 312-318, 2016.

9. Gu, L., Li, L., Zhao, W., Rajurkar, K.P. Electrical discharge machining of Ti6Al4V with a bundled electrode. *Int. J. Mach. Tool. Manu.* Vol. 53, No. 1, pp. 100-106, 2012.
10. Song, K., Chung, D., Park, M., Chu, C. Electrical discharge machining using a strip electrode. *Precis. Eng.* Vol.37, No. 3, pp. 738-745, 2013.
11. Takino, H., Hosaka, T. Shaping of steel mold surface of lens array by electrical discharge machining with spherical ball electrode, *Appl. Opt.* Vol. 55, pp. 4967-4973, 2016.
12. Jiang, K., Wu, X., Lei, J., Hu, Z., Diao, D. Investigation on the geometric evolution of microstructures in EDM with a composite laminated electrode. *J. Clean. Prod.* Vol. 298, pp. 126765, 2021.
13. Zhang, Z., Yu, H., Zhang, Y., Yang, K., Li, W., Chen, Z. Analysis and optimization of process energy consumption and environmental impact in electrical discharge machining of titanium superalloys. *J. Clean. Prod.* Vol. 198, pp. 833-846, 2018.
14. Zhou, T., Zhou, C., Liang, Z., Wang, X. Machining mechanism in tilt electrical discharge milling for lens mold. *Int. J. Adv. Manuf. Tech.* Vol. 95, pp. 2747-2755, 2018.